Available online at www.sciencedirect.com
SCIENCE DIRECT®
Physica E 22 (2004) 554–557
PHYSICA E
www.elsevier.com/locate/physe

Kondo effect of an antidot in the integer quantum Hall regime: a microscopic calculation

H.-S. Sim[a,*], N.Y. Hwang[b], M. Kataoka[c], Hangmo Yi[a], M.-S. Choi[b], S.-R. Eric Yang[b]

[a] *School of Physics, Korea Institute for Advanced Study, 207-43 Cheongryangri-dong, Dongdaemun-gu, Seoul 130-722, South Korea*
[b] *Department of Physics, Korea University, 1 5-ka Anam-dong, Seoul 136-701, South Korea*
[c] *Cavendish Laboratory, Madingley Road, Cambridge CB3 0HE, UK*

Abstract

An electron antidot system is an open geometry problem and often requires heavy calculations to compute its physical properties. Such a difficulty can be avoided by transforming an electron antidot system to a system of hole quantum dot since the transformed system contains only a finite number of confined holes. Using this transformation, we present a microscopic approach to study electronic properties of an antidot in the integer quantum Hall regime. Based on this approach we discuss various conditions under which the Kondo effect may be present.

PACS: 73.43.−f; 72.15.Qm

Keywords: Antidot; Quantum Hall effect; Kondo effect

1. Introduction

A quantum antidot is a potential hill in two dimensional electron gas (2DEG) systems [1–8]. It can be formed in GaAs/AlGaAs heterostructures by applying a gate potential or making an etched pit. In zero magnetic field, it is a simple repulsive potential and acts as a scattering center for electrons. However, when a strong magnetic field is applied perpendicular to 2DEG, the antidot has its own electronic "edge" structures, which correspond to classical skipping orbits around the antidot resulting from the Lorentz force. When they are weakly coupled to extended edge channels along the boundary of 2DEG, these localized antidot structures provide resonant states, giving rise to Aharonov–Bohm oscillations of conductance [3–8].

Electron–electron interactions may significantly affect the localized antidot states, as in the extended edge channels [9–11]. Indeed, the charging effect [3,4,6], $h/(2e)$ Aharonov–Bohm oscillations [7], and Kondo-like signatures [8], all of which cannot be understood within a single-particle picture, have been observed in transport measurements of the antidot systems. In spite of these experimental efforts, there have been few theoretical works to understand the interaction effects. Very recently, a capacitive interaction model has been proposed [12] to explain the experimental results. This model is analogous to the constant interaction model of quantum dots [13]. In

* Corresponding author.
E-mail address: hssim@kias.re.kr (H.-S. Sim).

1386-9477/$ - see front matter © 2003 Elsevier B.V. All rights reserved.
doi:10.1016/j.physe.2003.12.068

this model, the capacitive couplings between localized excess charges, which are formed around the antidot due to magnetic flux quantization, result in Coulomb blockade and nontrivial Aharonov–Bohm oscillations with Kondo resonances. The predicted results are in good qualitative agreement with the experimental observations [7,8].

In this paper, we present a microscopic approach to study the effect of electron–electron interactions in antidots. In this approach, we map the electron antidot system into a hole quantum dot system and perform a Hartree–Fock calculation. We calculate, as a function of magnetic field, the chemical potential for about 50 holes. We find transitions between maximum density droplets [14–16], which may lead to Kondo resonances [17,18] in the electron antidot system. Types of changes in many-body states depend on the shape of the antidot potential. Although several hundreds of holes are required to directly compare the result of the Hartree–Fock calculation with those of the transport measurements and the theoretical capacitive interaction model, our results indicate that the Kondo effect may exist in an antidot system with two localized edge states.

2. Particle–hole transformation

Although there are many microscopic calculations of quantum dots, to our knowledge, no microscopic study of quantum antidots exists. It might be because the electron antidot system is an open geometry and requires heavy calculations. Such a difficulty can be avoided by transforming an electron antidot system to a hole quantum dot (see Fig. 1). Then the transformed system contains only a finite number of confined holes which makes it possible to perform a microscopic calculation.

We first describe our model for an isolated antidot electron system, which is decoupled to the external edge channels. Electrons reside in the xy plane and a magnetic field $\boldsymbol{B} = B\hat{z}$ is applied perpendicular to the plane. For simplicity, we choose an antidot potential $V(r)$, which has a rotational symmetry along the $\hat{z}$ axis (the detailed shape of $V(r)$ will be mentioned later). Following the experimental setup [7,8], we will assume that the antidot has only two edge states with different spins, which come from

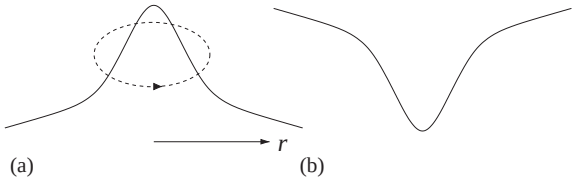

Fig. 1. (a) Schematic diagram of an antidot potential with a circulating localized electron orbit (dashed arrow). The potential will be transformed into a confinement potential drawn in (b) by a particle–hole mapping.

the lowest Landau-level. The Landau-level mixing effects can be neglected when the Landau-level spacing $\hbar\omega_c$ ($\equiv \hbar eB/m^*$) is comparable to or larger than the interaction energy scale of $e^2/\varepsilon l_B$ and when the antidot potential $V(r)$ is sufficiently slowly varying (m^* is the electron effective mass, ε is the dielectric constant, and $l_B \equiv \sqrt{\hbar/eB}$ is the magnetic length). In our calculation the Landau-level mixing is ignored, and in a symmetric gauge the lowest Landau-level single-particle antidot state $\phi_{m\sigma}(r,\theta)$ can be labeled by two quantum numbers, the orbital angular momentum $m = 0, 1, 2, \ldots$ and spin index $\sigma = \uparrow, \downarrow$. The single-particle energy of $\phi_{m\sigma}$ is $e_{m\sigma} = \left(\frac{1}{2}\right)\hbar\omega_c + V_m + E_{Z\sigma}$ where $V_m = \langle\phi_{m\sigma}|V(r)|\phi_{m\sigma}\rangle$ and $E_{Z\uparrow} = -\left(\frac{1}{2}\right) g\mu_B B$ ($E_{Z\downarrow} = \left(\frac{1}{2}\right) g\mu_B B$) is the Zeeman energy of spin-up(down) electrons. The wave function $\phi_{m\sigma}(r,\theta)$ is centered at $r = r_m \equiv \sqrt{2(m+1)}l_B$, and has the width of l_B.

The Hamiltonian of the many-body antidot states can be written as

$$H = \sum_{m\sigma} e_{m\sigma} c^\dagger_{m\sigma} c_{m\sigma} + \sum_{m_1 m_2 m_1' m_2' \sigma_1 \sigma_2} U_{m_1' m_2'; m_1 m_2} c^\dagger_{m_2'\sigma_2} c^\dagger_{m_1'\sigma_1} c_{m_1\sigma_1} c_{m_2\sigma_2} - \sum_{m\sigma} V^{\text{ion}}_m c^\dagger_{m\sigma} c_{m\sigma}, \quad (1)$$

where $c^\dagger_{m\sigma}$ creates an electron in the single-particle state $\phi_{m\sigma}$ and $U_{m_1' m_2'; m_1 m_2}$ is the matrix element describing Coulomb interaction; each element of U has the half value of the corresponding element of the Coulomb matrix. Whenever $m_1' + m_2' \neq m_1 + m_2$, $U_{m_1' m_2'; m_1 m_2}$ is zero. The last term (V^{ion}_m) of Eq. (1) represents the interaction with the positive background.

Since there are as many ions as spin-up and -down electrons, one obtains $V_m^{\rm ion} = 4\sum_{m'} U_{mm';mm'}$.

The particle-hole transformation from the anti-dot electron system into a hole quantum dot can be achieved by the mapping [19] $c_{m\sigma} \to h_{m\sigma}^\dagger$ and $c_{m\sigma}^\dagger \to h_{m\sigma}$, where $h_{m\sigma}^\dagger$ ($h_{m\sigma}$) is the hole creation (annihilation) operator. Since the transformed system confines a finite number N of holes, one can use a cut-off angular momentum $m_c \gg N$. After the mapping, the last term in Eq. (1) is transformed into

$$-\sum_{m\sigma}^{m_c} V_m^{\rm ion} c_{m\sigma}^\dagger c_{m\sigma} = 2\sum_m^{m_c} V_m^H \left(-2 + \sum_\sigma h_{m\sigma}^\dagger h_{m\sigma}\right),$$

where $V_m^H \equiv 2\sum_{m'}^{m_c} U_{mm';mm'}$. The transformed total hole Hamiltonian can be obtained as

$$H_h = \sum_{m\sigma}^{m_c} \tilde{e}_{m\sigma} h_{m\sigma}^\dagger h_{m\sigma} + \sum_{m_1 m_2 m_1' m_2' \sigma_1 \sigma_2}^{m_c} U_{m_1' m_2';m_1 m_2} h_{m_2\sigma_2}^\dagger h_{m_1\sigma_1}^\dagger h_{m_1'\sigma_1} h_{m_2'\sigma_2} + \sum_{m\sigma}^{m_c} e_{m\sigma} - \sum_m^{m_c} (2V_m^H + V_m^X), \quad (2)$$

where $V_m^X \equiv 2\sum_{m'}^{m_c} U_{mm';m'm}$ and the effective single hole energy is $\tilde{e}_{m\sigma} = -e_{m\sigma} + V_m^X$. Note that the Zeeman energy of holes has the opposite sign to that of electrons. The constant terms in H_h will be ignored hereafter.

3. Results and discussion

We choose a parabolic confinement potential $\left(\frac{1}{2}\right) m^* \omega_0^2 r^2$ for the hole quantum dot and put about $N \simeq 50$ holes into the dot. The potential energy of the electronic state $\phi_{m\sigma}$ is $V_m = -\gamma(m+1)$, where $\gamma = \hbar\omega_c(\omega_0/\omega_c)^2$. For $m^* = 0.067 m_e$, $\varepsilon = 10$, $g = 0.44$, $\omega_0 = 1.5$ meV, $N = 48$, and $B \sim 1$ T, we find that the maximum-density droplet [14–16] is the exact ground state of the hole Hamiltonian, Eq. (2). It can be written as a single-Slater-determinant state

$$|N_\downarrow, N_\uparrow\rangle = h_{(N_\downarrow-1)\downarrow}^\dagger \cdots h_{0\downarrow}^\dagger h_{(N_\uparrow-1)\uparrow}^\dagger \cdots h_{0\uparrow}^\dagger |0\rangle. \quad (3)$$

Here N_σ stands for the number of holes with spin σ. The total number of holes is $N = N_\uparrow + N_\downarrow$, and $N_\downarrow$ is equal to or larger than $N_\uparrow$ due to the Zeeman energy.

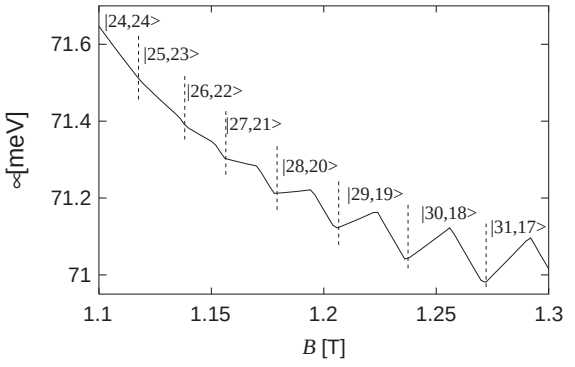

Fig. 2. Chemical potential $\mu_{N=48}$ of a hole quantum dot as a function of magnetic field B. Particles in the dot are confined in the parabolic potential $\left(\frac{1}{2}\right) m^* \omega_0^2 r^2$. The dashed lines indicate the values of B where the states $|N_\downarrow, N_\uparrow\rangle$ and $|N_\downarrow + 1, N_\uparrow - 1\rangle$ are degenerate.

We have investigated how the many-body ground states of the hole quantum dot change with varying magnetic field. Whenever the chemical potential satisfies the normal resonance condition $\mu_N = E_{N+1} - E_N = E_F$, an extra hole tunnels into the quantum dot. Here E_N and E_F are the ground state energy of N-particle system and the Fermi energy, respectively. At the normal resonance condition, a pair of states with N and $N+1$ holes, $|N_\downarrow, N_\uparrow\rangle$ and $|N_\downarrow + 1, N_\uparrow\rangle$, are degenerate and the ground state changes from $|N_\downarrow, N_\uparrow\rangle$ to $|N_\downarrow + 1, N_\uparrow\rangle$ as the magnetic field becomes stronger [12].

In addition to the ground state transition at the normal resonance conditions, there can appear another type of ground state transition, in which the total number N of holes does not vary and the ground state $|N_\downarrow, N_\uparrow\rangle$ changes into either $|N_\downarrow + 1, N_\uparrow - 1\rangle$ or $|N_\downarrow - 1, N_\uparrow + 1\rangle$ as the magnetic field increases. This type of transition accompanies a spin-flip process, indicating the possibility of the Kondo effect [20]. In the hole quantum dot with the parabolic potential, this spin-flip ground state transitions occur following the sequence $|N_\downarrow, N_\uparrow\rangle \to |N_\downarrow + 1, N_\uparrow - 1\rangle$ as B increases (see Fig. 2).

In the case of the parabolic potential, both at the spin-flip transitions of the sequence $|N_\downarrow, N_\uparrow\rangle \to |N_\downarrow + 1, N_\uparrow - 1\rangle$ and at the normal resonance conditions, the number of the spin-down holes becomes larger and thus the hole spin polarization ($\propto N_\uparrow - N_\downarrow$)

decreases as B increases; note that decreasing hole spin polarization is equivalent to increasing electron spin polarization. However, this result does not match those expected in the experiment [8] of large-size realistic antidots and the results of the capacitive interaction model [12]. In large-size antidots, it is naturally expected that the spin polarization would show a periodic oscillation with Aharonov–Bohm period in a wide range of magnetic field (at least in several Aharonov–Bohm periods). Consistent with this expectation the capacitive interaction model predicts the transition sequence of $|N_\downarrow, N_\uparrow\rangle \rightarrow |N_\downarrow - 1, N_\uparrow + 1\rangle$ with increasing B at the Kondo resonances.

The discrepancy may be due to the possibilities that the inverse parabolic potential cannot describe the realistic antidot potential and/or that the number $N \simeq 50$ of holes is one-order smaller than the value expected in the experimental situation. To test the former possibility, we also performed [12] the calculation for a bell-shape antidot potential, which is more realistic, and found the spin-flip transition of the correct sequence with $|N_\downarrow, N_\uparrow\rangle \rightarrow |N_\downarrow - 1, N_\uparrow + 1\rangle$. The test of the second possibility with much more holes is now in progress. Finally, we remark that the realistic antidot state may be either alternating compressible and incompressible regions [9,15] or a maximum-density droplet [14–16] of holes. This interesting issue may also be solved in the calculation for the antidot system with a realistic size.

References

[1] S.W. Hwang, J.A. Simmoons, D.C. Tsui, M. Shayegan, Phys. Rev. B 44 (1991) 13497.

[2] D. Weiss, M.L. Roukes, A. Menschig, P. Grambow, K. von Klitzing, G. Weimann, Phys. Rev. Lett. 66 (1991) 2790.

[3] C.J.B. Ford, P.J. Simpson, I. Zailer, D.R. Mace, M. Yosefin, M. Pepper, D.A. Ritchie, J.E.F. Frost, M.P. Grimshaw, G.A.C. Jones, Phys. Rev. B 49 (1994) 17456.

[4] A.S. Sachrajda, Y. Feng, R.P. Taylor, G. Kirczenow, L. Henning, J. Wang, P. Zawadzki, P.T. Coleridge, Phys. Rev. B 50 (1994) 10856.

[5] V.J. Goldman, B. Su, Science 267 (1995) 1010.

[6] M. Kataoka, C.J.B. Ford, G. Faini, D. Mailly, M.Y. Simmons, D.R. Mace, C.-T. Liang, D.A. Ritchie, Phys. Rev. Lett. 83 (1999) 160.

[7] M. Kataoka, C.J.B. Ford, G. Faini, D. Mailly, M.Y. Simmons, D.A. Ritchie, Phys. Rev. B 62 (2000) R4817.

[8] M. Kataoka, C.J.B. Ford, M.Y. Simmons, D.A. Ritchie, Phys. Rev. Lett. 89 (2002) 226803.

[9] D.B. Chklovskii, B.I. Shklovskii, L.I. Glazman, Phys. Rev. B 46 (1992) 4026.

[10] C.d.C. Chamon, X.G. Wen, Phys. Rev. B 49 (1994) 8227.

[11] J.H. Oaknin, L. Martín-Moreno, C. Tejedor, Phys. Rev. B 54 (1996) 16850.

[12] H.-S. Sim, M. Kataoka, Hangmo Yi, N.Y. Hwang, M.-S. Choi, S.-R. Eric Yang, Phys. Rev. Lett. 91 (2003) 266801.

[13] L.I. Glazman, M. Pustilnik, condmat/0302159.

[14] S.-R.E. Yang, A.H. MacDonald, M.D. Johnson, Phys. Rev. Lett. 71 (1993) 3194;
A.H. MacDonald, S.-R.E. Yang, M.D. Johnson, Aust. J. Phys. 46 (1993) 345.

[15] S.-R.E. Yang, A.H. MacDonald, Phys. Rev. B 66 (2002) 41304(R).

[16] O. Klein, C.de C. Chamon, D. Tang, D.M. Abusch-Magder, U. Meirav, X.-G. Wen, M.A. Kastner, Phys. Rev. Lett. 74 (1995) 785;
T.H. Oosterkamp, J.W. Janssen, L.P. Kouwenhoven, D.G. Austing, T. Honda, S. Tarucha, Phys. Rev. Lett. 82 (1999) 2931.

[17] J. Kondo, Prog. Theor. Phys. 32 (1964) 37.

[18] A.C. Hewson, The Kondo Problem to Heavy Fermions, Cambridge University Press, Cambridge, 1993.

[19] M.D. Johnson, A.H. MacDonald, Phys. Rev. Lett. 67 (1991) 2060.

[20] M.S. Choi, N.Y. Hwang, S.-R. Eric Yang, condmat/0212577; Phys. Rev. B 67 (2003) 245323.